

Vanillic acid promotes keratinocyte migration, proliferation, and angiogenesis

Xianfeng Zhu¹, Jiangyun Ma^{2*}, Jian Huang²

¹Intensive Care Unit, Hangzhou Ninth People's Hospital, Hangzhou, Zhejiang, China; ²Department of Emergency, Hangzhou Ninth People's Hospital, Hangzhou, Zhejiang, China

***Corresponding Author:** Jiangyun Ma, Department of Emergency, Hangzhou Ninth People's Hospital, No. 98, Yilong Road, Yipeng Street, Qiantang District, Hangzhou, Zhejiang, China. Email: majiangyun821@163.com

Received: 16 August 2024; Accepted: 25 September 2024; Published: 26 September 2024

© 2024 Codon Publications

OPEN ACCESS



ORIGINAL ARTICLE

Abstract

Wound healing is a complex, multi-phase process involving the coordinated interaction of various cells and molecules. This study evaluates the effects of vanillic acid (VA) on wound healing using HaCaT cells. The results demonstrate that VA treatment increases the levels of phosphorylated AMPK protein, thereby activating the AMPK pathway. This activation leads to an upregulation of PNCA expression and enhances the proliferation of HaCaT cells. Additionally, VA treatment reduces the expression of Bax and cleaved Caspase-3 while increasing Bcl2 expression, which inhibits apoptosis in HaCaT cells. Furthermore, VA treatment upregulates the expression of MMP-2 and MMP-9, promoting HaCaT cell migration. VA also induces the secretion of FGF, VEGF, and PDGF, which enhances tube formation in HUVECs. In conclusion, VA may have potential therapeutic benefits in wound healing by promoting keratinocyte proliferation, migration, and angiogenesis.

Keywords: keratinocyte migration; NF- κ B pathway; proliferation and angiogenesis; vanillic acid; wound healing

Introduction

Wound healing progresses through several distinct phases, including hemostasis, inflammation, epithelialization, granulation tissue formation, matrix deposition, and tissue remodeling, with the ultimate goal of restoring both the structural integrity and functional capacity of the injured tissues (Gonzalez *et al.*, 2016). A key indicator of successful wound healing is the complete reconstruction of the epidermal barrier. Re-epithelialization, which involves the migration, proliferation, and resurfacing of epithelial cells, particularly keratinocytes, is a crucial and decisive aspect of this process (Rousselle *et al.*, 2019). During re-epithelialization, epithelial cells, forming the outer layer of the skin, migrate toward the wound, proliferate, and cover the damaged area (Pastar *et al.*, 2014). Keratinocytes, as a subset of epithelial cells,

play a vital role in regenerating the skin's outermost layer (Fang & Lan, 2023; Rakita *et al.*, 2020) and are thus essential for effective wound healing (Dekoninck & Blanpain, 2019).

VA is an aromatic carboxylic acid known for its diverse therapeutic potential, attributed to its various biochemical properties (Kaur *et al.*, 2022). VA exhibits a range of physiological functions, including anti-inflammatory, antimicrobial, antioxidant, and anticancer activities (Gong *et al.*, 2019; Ma *et al.*, 2020; Qian *et al.*, 2020; Salau *et al.*, 2020). In the context of myocardial health, VA has been shown to enhance myocardial cell vitality, reduce apoptotic cell percentages, and restore mitochondrial membrane potential by increasing levels of Adenosine Monophosphate-Activated Protein Kinase $\alpha 2$ (AMPK $\alpha 2$), thereby mitigating myocardial injury

caused by hypoxia/reoxygenation (Yao *et al.*, 2020). Regarding respiratory health, VA can inhibit the inflammatory response in an ovalbumin (OVA)-induced asthma rat model, thereby alleviating asthma symptoms (Bai *et al.*, 2019). Additionally, VA has shown promise in the treatment of allergic inflammatory diseases by inhibiting caspase-1 and NF- κ B activity in mast cells, leading to the suppression of inflammatory responses (Jeong *et al.*, 2018). Furthermore, it has also been reported that fruit extracts, including VA, can protect the skin by inhibiting oxidative stress and reducing stress-induced MAPK responses, which collectively counteract UVB-induced damage to keratinocytes (Natewong *et al.*, 2022).

Despite these promising therapeutic properties in various diseases, limited information is available regarding the potential role of VA in wound healing. Therefore, this study aims to investigate the function and mechanisms of VA, potentially offering a novel therapeutic strategy for enhancing wound healing.

Materials and Methods

Cell models

HaCaT cells, obtained from the National Biomedical Cell-Line Resource Center (BMCR), were used to investigate the influence of VA on wound healing. These cells, which retain essential characteristics similar to primary keratinocytes, were cultured in DMEM medium (Gibco, Code No. 11965092) supplemented with 10% FBS (Gibco, Code No. 10099141C) at a density of 1×10^5 cells/mL. HaCaT cells were divided into four groups: a control group without VA treatment, a low-concentration group treated with 25 μ g/mL VA, a medium-concentration group treated with 50 μ g/mL VA, and a high-concentration group treated with 100 μ g/mL VA. To investigate VA's impact on the AMPK pathway, HaCaT cells were further divided into three groups: a control group without VA treatment, a VA (100 μ g/mL) treatment group, and a VA (100 μ g/mL) plus compound c (CC, AMPK inhibitor) co-treatment group.

Cell proliferation assay by Cell Counting Kit-8 (CCK-8)

HaCaT cells were plated in 96-well plates at a density of 10,000 cells/well and subjected to various concentrations of VA or co-treated with VA and CC for 0, 24, 48, and 72 h. Cell proliferation was performed based on the provided kit manual (Beyotime, Code No. C0009M). Absorbance was measured at 570 nm using a Multiskan FC instrument (ThermoFisher).

Cell proliferation assay by EdU/DAPI staining (detection of S-phase)

To evaluate the proliferation of HaCaT cells, the BeyoClick™ EdU Cell Proliferation Kit (Beyotime, Code No. C0081S) was used in conjunction with DAPI Staining Solution (Beyotime, Code No. C1005). HaCaT cells were seeded in 96-well plates at a density of 10,000 cells per well and treated with varying concentrations of VA. Following treatment, the cells were incubated with an EdU working solution. Afterward, the medium was removed, and the cells were fixed, permeabilized, and washed. Subsequently, the cells were stained with DAPI solution. Images of five fields of view were captured, and the average cell count was determined. The proliferation rate was calculated as the ratio of EdU-positive (proliferating) cells to DAPI-positive (total) cells.

Apoptosis assay

To assess apoptosis in HaCaT cells, we used the Annexin V-FITC Apoptosis Detection Kit (Beyotime, Code No. C1062L). Briefly, the cells were digested with a 0.05% trypsin solution (Gibco, Code No. 25300054), collected, and washed with PBS. Cell counting was performed, and the cell concentration was adjusted to approximately 1×10^6 cells/mL. Annexin V-FITC and PI were then sequentially added to the cell suspension, which was mixed gently and incubated in the dark. Apoptosis was analyzed by flow cytometry (FACS) within 1 h. Healthy cells were identified as Annexin V-/PI-, early apoptotic cells as Annexin V+/PI-, late apoptotic cells as Annexin V+/PI+, and necrotic cells as Annexin V-/PI+.

Detection of cell migration by scratch assay

The scratch assay, a commonly used method for studying cell migration and wound healing, was employed in this study. HaCaT cells were cultured in 6-well plates for 24 h until a confluent monolayer was established. A sterile pipette tip was then used to create a scratch in the monolayer. Following the scratch, the cells were gently washed to remove any floating cells or debris. The culture medium was replaced, and the cells were incubated for an additional 24 h. Images were captured immediately after creating the scratch and at the end of the 24-h incubation period. The width of the scratch was measured using ImageJ software to assess cell migration.

Detection of angiogenesis by tube formation assay

The tube formation assay is a widely recognized method for assessing angiogenesis in vitro. Briefly, HaCaT cells

were exposed to VA for 24 h, and the resulting conditioned medium (CM) was used for the assay. HUVECs were cultured in DMEM/F12 medium (Gibco, Code No. 11320033) supplemented with 10% FBS (Gibco, Code No. 10099141C). A 96-well plate was pre-coated with 50 μ L of Matrigel (Corning, Code No. 354230) and incubated at 37°C for 30 min to allow Matrigel solidification. HUVEC cells were then seeded onto the Matrigel-coated 96-well plates at a density of 10,000 cells/well. Once cell adhesion to the Matrigel was established, the culture medium was replaced with either the CM or a control medium. The cells were then cultured for an additional 24 h, and their angiogenic activity was observed under a microscope. Images from five different fields of view were captured, and the number of tubes formed was quantified using image analysis software.

Determination of FGF, VEGF, and PDGF release by ELISA kits

To measure the levels of FGF, VEGF, and PDGF, HaCaT cells subjected to various treatments were centrifuged to collect the culture supernatants. The quantification of these factors was performed using the following ELISA kits: Human FGF basic Quantikine ELISA Kit (R&D Systems, Code No. DFB50), Human VEGF Quantikine ELISA Kit (R&D Systems, Code No. DVE00), and Human PDGF-BB Quantikine ELISA Kit (R&D Systems, Code No. DBB00).

Determination of protein expression by western blotting assay

Total proteins from HaCaT cells were obtained using RIPA buffer (Beyotime, Code No. P0013B), which includes several inhibitors to effectively prevent protein degeneration during sample lysis. The total proteins were then separated through electrophoresis using 8% SDS-PAGE gels. The primary antibodies and their respective dilution ratios were as follows: β -actin (Clone 15G5A11/E2, Invitrogen, Code No. MA1-140, 1:5,000), PCNA (Clone PC10, Invitrogen, Code No. 14-9910-82, 1:1,000), Bax (Clone 6A7, Invitrogen, Code No. 14-6997-82, 1:1,000), cleaved Caspase-3 (Clone E83-77, Abcam, Code No. ab32042, 1:10,000), Bcl2 (Clone Bcl-2/100, Invitrogen, Code No. BMS1028), cleaved Caspase-9 (Invitrogen, Code No. PA5-17913, 1:5,000), BAD (Clone Y208, Abcam, Code No. ab32445, 1:5,000), MMP-2 (Clone 101, Invitrogen, Code No. 436000, 1:500), MMP-9 (Clone JA80-73, Invitrogen, Code No. MA5-32705, 1:1,000), AMPK (Clone 9Q34, Invitrogen, Code No. AHO1332, 1:500), and Phospho-AMPK (Clone 10H2L20, Invitrogen, Code No. 701068, 1:500). An image analysis software was used to assess the relative levels of PCNA,

Bax, cleaved Caspase-3, Bcl2, MMP-2, MMP-9, AMPK, and phospho-AMPK.

Statistical analyses

Statistical assessment were performed using GraphPad Prism (version 9.4.1) and Flow cytometry data were analyzed using FlowJo (version 10.8.1). Scratch width measurements were performed using ImageJ software. Tube formation quantification was carried out with microscope software. Semi-quantitative analysis of western blotting results was performed using ImageJ software. Each data point represents the mean of three replicates, expressed as mean \pm SD.

Results

VA promoted keratinocyte proliferation

The effects of VA on HaCaT cell proliferation were assessed using the MTT assay (Figure 1A). Compared to non-treated HaCaT cells, proliferation at various time points with 25 μ g/mL VA was similar ($P > 0.05$). However, at 48 and 72 h, significant enhancement in HaCaT cell proliferation was observed with 50 and 100 μ g/mL VA. The proliferating HaCaT cells were subsequently identified and quantified through EdU/DAPI staining (Figure 1B). The percentage of EdU-positive HaCaT cells exhibited a 3- to 4-fold increase in the 50 and 100 μ g/mL VA treatment groups, whereas no significant increase was observed in the 25 μ g/mL VA treatment group. These findings were consistent with the MTT assay results. Furthermore, the expression of proliferating cell nuclear antigen (PCNA) was examined to assess DNA replication activity (Figure 1C). Western blot results revealed upregulation of PCNA expression in all three VA treatment groups, with the effect being dose-dependent. Collectively, these results demonstrate that HaCaT cell proliferation was significantly enhanced with medium- to high-concentration VA treatment.

VA inhibited keratinocyte apoptosis

The influence of VA on the apoptotic rates of HaCaT cells was assessed and quantified using Annexin V/PI (Figure 2A). Flow cytometry results indicated an apoptosis ratio of approximately 20% in the absence of VA treatment. However, VA treatment significantly reduced the percentage of apoptotic cells, particularly those that were Annexin V-FITC+/PI-. With 100 μ g/mL VA treatment for 24 h, the apoptosis ratio decreased to approximately 5%. The impact of VA on HaCaT cell apoptosis was further investigated by examining the expression

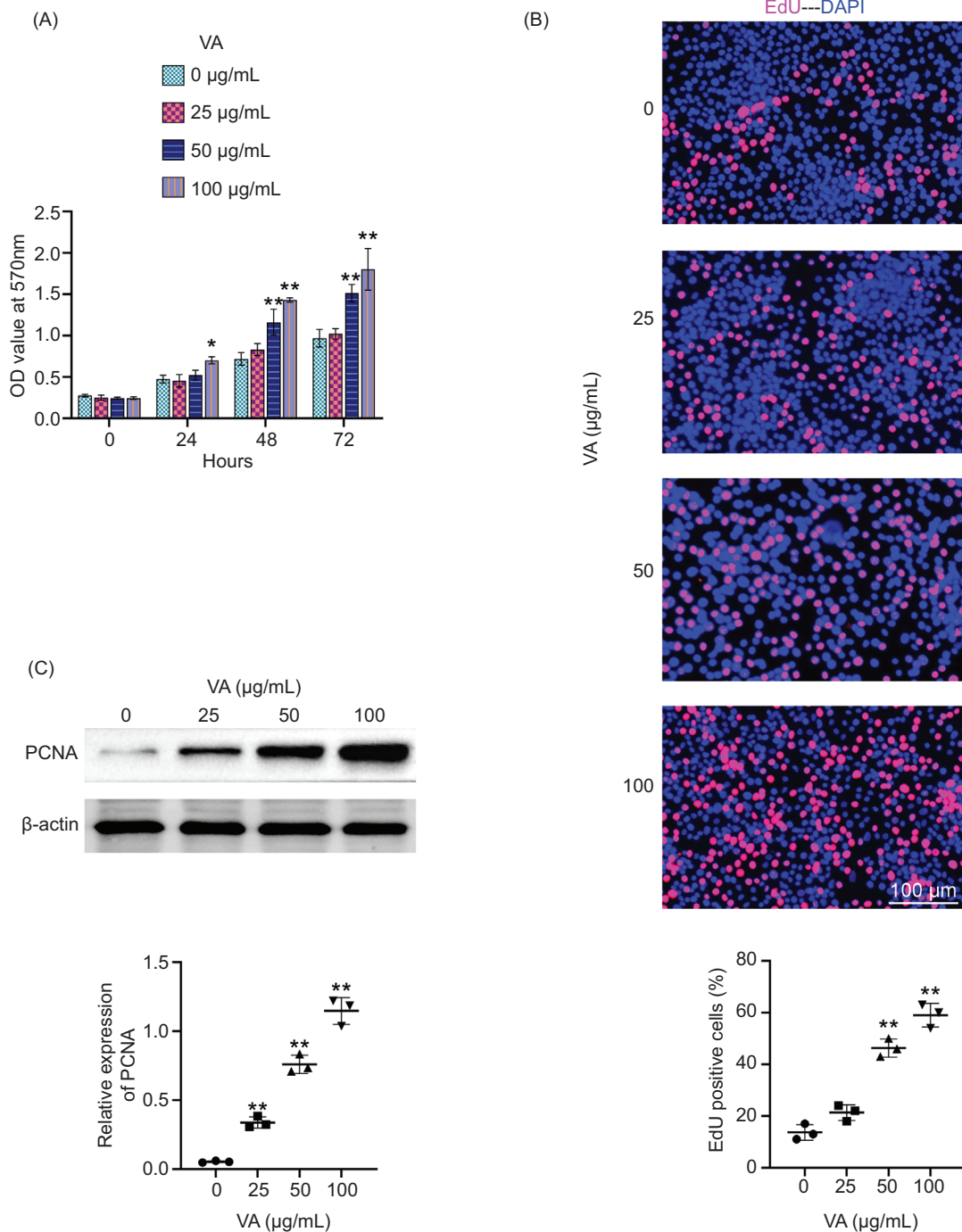


Figure 1. VA promotes the proliferation of keratinocytes. (A) The proliferation of HaCaT cells was measured using the MTT assay. OD₅₇₀ values were measured at 0, 24, 48, and 72 h. (B) Proliferating HaCaT cells were identified and quantified by EdU/DAPI staining at 24 h. (C) The expression of PCNA was detected by western blotting at 24 h. HaCaT cells were treated with 0, 25, 50 and 100 $\mu\text{g/mL}$ VA. * $p < 0.05$, ** $p < 0.01$ vs. 0 $\mu\text{g/mL}$ VA group.

of apoptosis-related proteins, including Bax, Bcl2, and cleaved Caspase-3 (Figure 2B). Treatment with 25, 50 and 200 $\mu\text{g/mL}$ VA downregulated pro-apoptotic protein Bax, upregulated the anti-apoptotic protein Bcl2 expressions, and reduced the levels of cleaved Caspase-3, cleaved Caspase-9, and BAD. However,

HaCaT cells treated with 25 $\mu\text{g/mL}$ VA exhibited minimal changes in Bax, Bcl2, and cleaved Caspase-3 expression, which was consistent with the findings from Annexin V/PI staining. These results suggest that medium- to high-concentration VA effectively inhibits apoptosis in HaCaT cells.

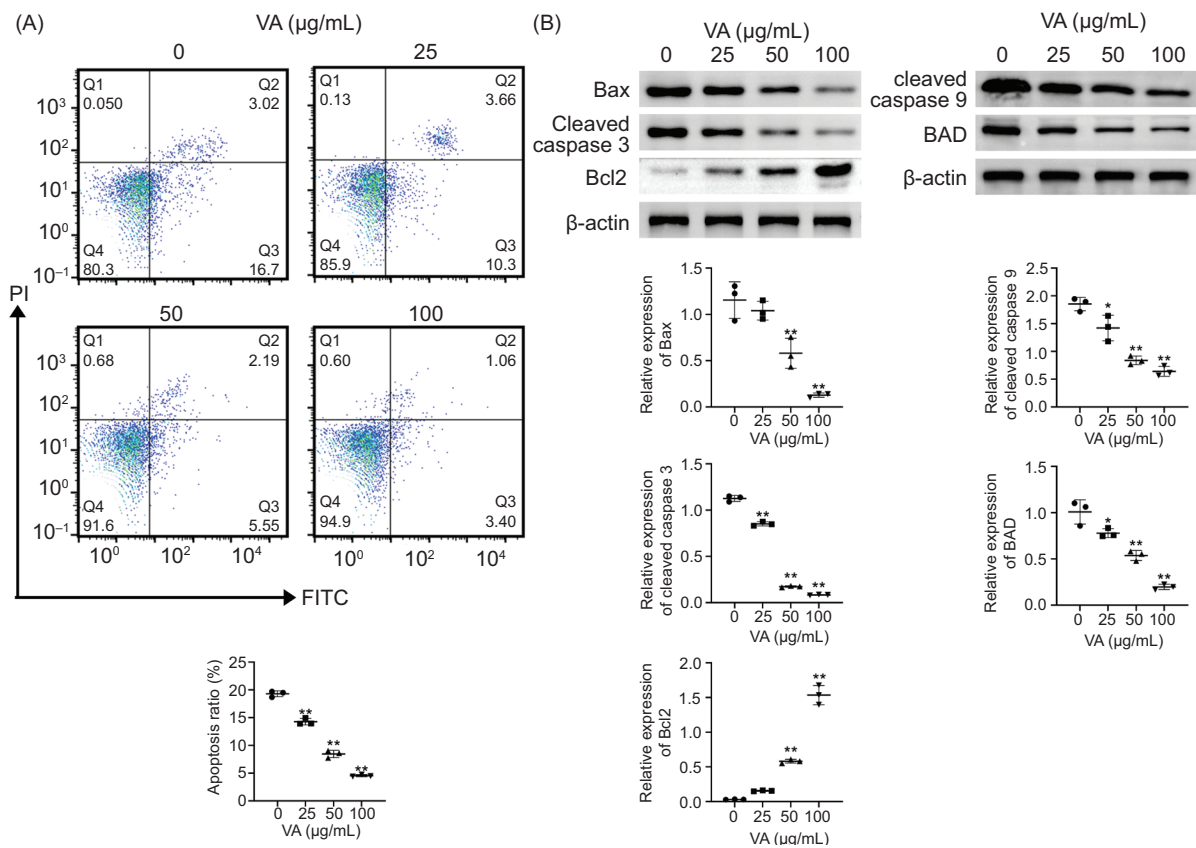


Figure 2. VA inhibits the apoptosis of keratinocytes. (A) Flow cytometry analysis of HaCaT cell apoptosis was performed using Annexin V-FITC/ PI staining at 24 h. Annexin V-/PI- represents healthy cells, Annexin V+/PI- represents early apoptotic cells, Annexin V+/PI+ represents late apoptotic cells, and Annexin V-/PI+ represents necrotic cells. (B). The expression of Bax, Bcl2, and cleaved Caspase-3 was detected by western blotting. β-actin was used as the reference protein. A semi-quantitative analysis of Bax, Bcl2, and cleaved Caspase-3 expression was performed using ImageJ software. ** $p < 0.01$ vs. 0 µg/mL VA group.

VA promoted the migration of keratinocytes

The initial wound width and the width at 24 h were compared (Figure 3A). As expected, HaCaT cells without VA treatment exhibited relatively slow migration. A slight reduction in the scratch distance ratio was observed with 25 µg/mL VA treatment. In contrast, HaCaT cells treated with 100 µg/mL VA displayed a substantial enhancement in migration rate compared to the control, indicating that VA promotes cell migration. During cell migration, the secretion of matrix metallo-peptidases (MMPs) is triggered, leading to their localization at the leading edge of migrating cells, where they degrade the surrounding extracellular matrix (ECM) peptides. The expression of MMP-2 and MMP-9 was assessed through western blotting (Figure 3B), which showed that VA treatment significantly stimulated the expression of both MMP-2 and MMP-9 in HaCaT cells, with an increase of over 10-fold observed with 100 µg/mL VA treatment.

VA-treated HaCaT cell cultured medium induced tube formation in HUVECs

The tube formation assay in HUVECs was used to assess the effects of VA on angiogenesis. After VA treatment, the CM was collected, and the number of tube-like structures formed by HUVEC cells was compared to the control (Figure 4A). The CM from HaCaT cells cultured without VA treatment had minimal effect on tube-like structure formation, with only a few tubes observed. In contrast, CM from HaCaT cells treated with 25 µg/mL VA exhibited weak induction of tube formation. However, CM from HaCaT cells treated with 50 and 100 µg/mL VA significantly stimulated tube formation in HUVECs, resulting in a 5-fold increments in tube number compared to the control. Fibroblast growth factor (FGF), platelet-derived growth factor (PDGF), and vascular endothelial growth factor (VEGF) are crucial proteins that play significant roles in angiogenesis. To investigate the mechanism by which VA promotes angiogenesis, the

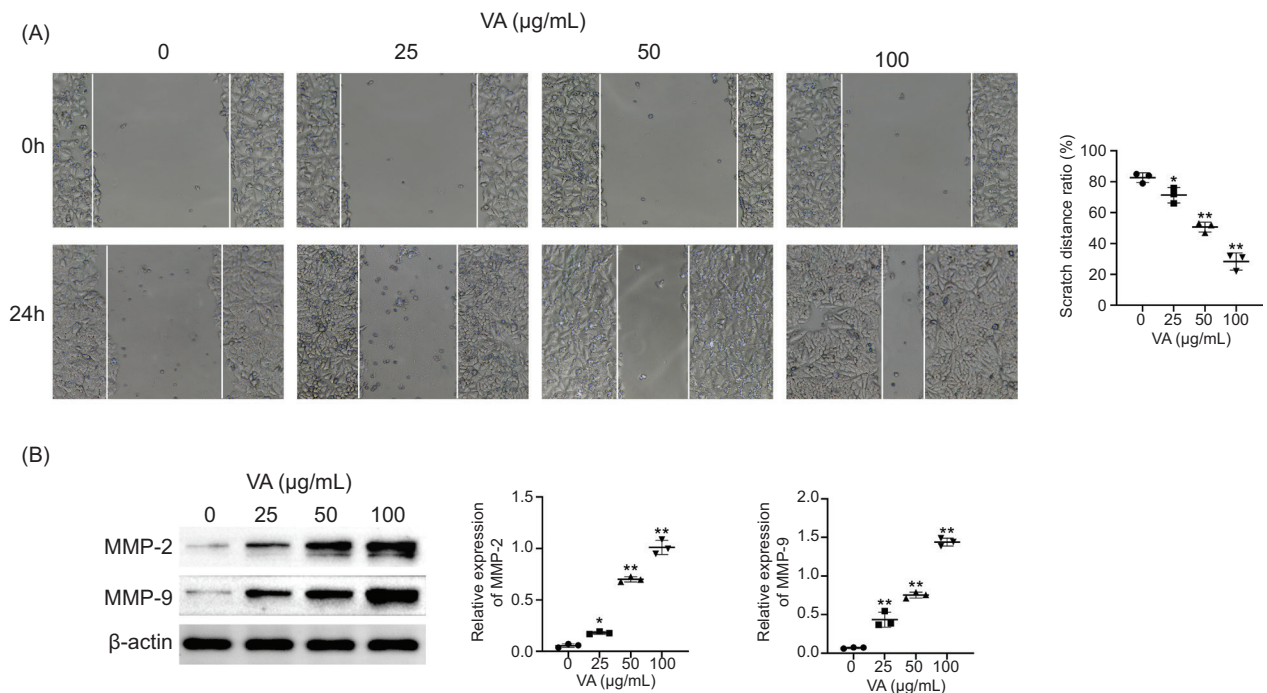


Figure 3. VA promotes the migration of keratinocytes. (A) The migration of HaCaT cells was evaluated using in vitro scratch assay. The width of the scratch was assessed using the ImageJ software. The scratch distance ratio was quantified by subtracting the width at 24 h from the width at T0 (immediately after scratch). (B) The expression of MMP-2 and MMP-9 was detected by western blotting. β-actin was used as the reference protein. Semi-quantitative analysis of MMP-2 and MMP-9 expression was calculated using image analysis software. * $p < 0.05$, ** $p < 0.01$ vs. 0 µg/mL VA group.

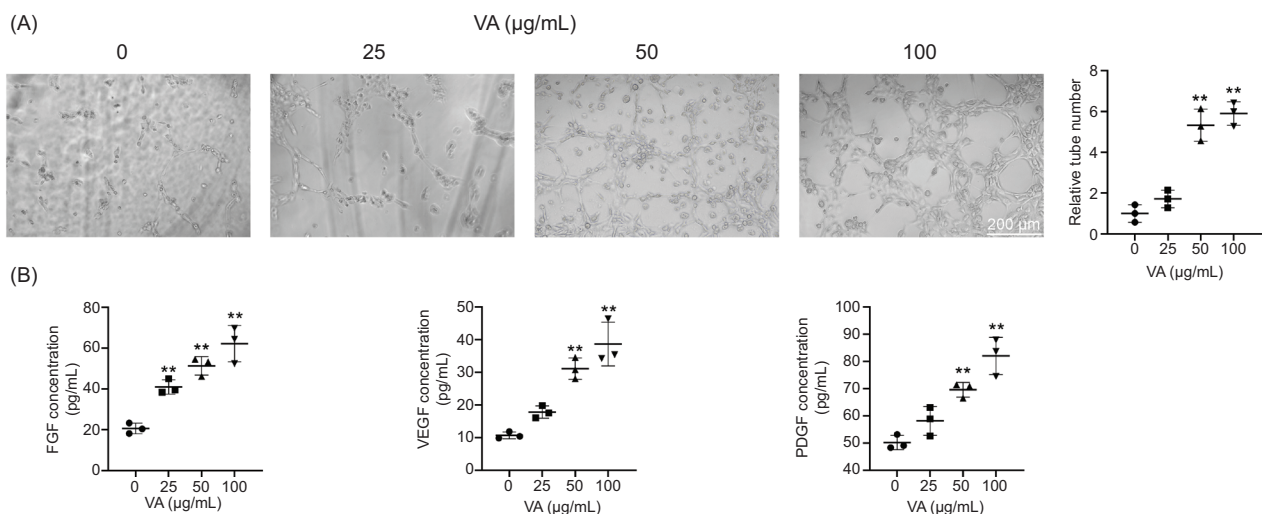


Figure 4. VA-treated HaCaT cell culture medium induces tube formation in HUVECs. (A) The impact of VA on angiogenesis processes was evaluated using a tube formation assay in HUVEC cells. The number of tubes was quantified using software and normalized to the control. (B) Secretion levels of FGF, PDGF, and VEGF were assessed using ELISA kits. ** $p < 0.01$ vs. 0 µg/mL VA group.

concentration of FGF, PDGF, and VEGF in the CM were assessed (Figure 4B). ELISA results demonstrated that VA treatment induced FGF and VEGF secretion by more than 3-fold, while PDGF secretion increased slightly, with a maximum fold increase of 1.6. These findings suggest that VA enhances angiogenesis by inducing the secretion of FGF and VEGF, thereby promoting tube formation in HUVECs.

VA affected keratinocytes by activating the AMPK pathway

The AMPK pathway plays a significant role in cell proliferation, migration, and angiogenesis, making it a crucial contributor to the wound healing process. Given that AMPK phosphorylation is a key event in activating this pathway, we assessed AMPK phosphorylation to explore the role of VA in AMPK pathway activation (Figure 5). In HaCaT cells cultured without VA treatment, the level of phosphorylated AMPK was low, indicating minimal activation of the AMPK pathway. However, treatment with 50 and 100 µg/mL VA resulted in a substantial increase in AMPK phosphorylation, with levels exceeding a 10-fold increase compared to the control. These results suggest that high concentrations of VA significantly activate the AMPK pathway.

To further validate whether VA indeed exerts its function through the activation of the AMPK pathway, an AMPK inhibitor compound, CC, was used. The effects of VA and CC co-treatment on HaCaT cell proliferation, apoptosis, migration, and angiogenesis were assessed (Figure 6A-E). Co-treatment with CC was found to significantly reverse the promotion of HaCaT cell proliferation and the upregulation of PCNA expression induced by 100 µg/mL VA treatment. The apoptosis ratio of HaCaT cells co-treated with 100 µg/mL VA and CC was nearly the same as

that of the control, indicating that CC also reversed the anti-apoptotic effect of VA. A similar reversal effect was observed in HaCaT cell migration. The AMPK inhibitor CC further reduced the secretion of FGF, VEGF, and PDGF to the control levels, indicating that the inhibition of the AMPK pathway could reverse the angiogenesis-promoting function of VA.

Discussion

Several pharmacological agents, such as antibiotics, anti-inflammatories, growth factors, and corticosteroids, have demonstrated efficacy in promoting wound healing, each with its distinct mechanism of action (Oluwole *et al.*, 2022). The exploration of new drugs with diverse mechanisms is of significant importance. VA has been recognized for its antioxidative, anti-inflammatory, and antimicrobial properties (Ullah *et al.*, 2020). In this study, HaCaT cells were used to examine the effects and mechanisms of vanillic acid (VA) on keratinocyte proliferation, apoptosis, and migration. The findings suggest that VA has potential therapeutic benefits for wound healing.

Keratinocytes are fundamental for wound healing (Hegde *et al.*, 2021). In this study, VA significantly stimulated DNA synthesis in HaCaT cells, leading to an increase in S-phase cells and promoting cell proliferation. However, low doses of VA had minimal effects on keratinocyte proliferation, consistent with its influence on cell apoptosis. High doses of VA reduced the expression of pro-apoptotic proteins Bax and cleaved Caspase-3 while increasing the expression of the anti-apoptotic protein Bcl2. Consequently, VA treatment reduced early apoptosis of keratinocytes. The ECM provides structural support to cells but also acts as a barrier. Thus, ECM degradation is a necessary step in cell migration (Cabral-Pacheco *et al.*, 2020). Both MMP-2 and MMP-9 are associated

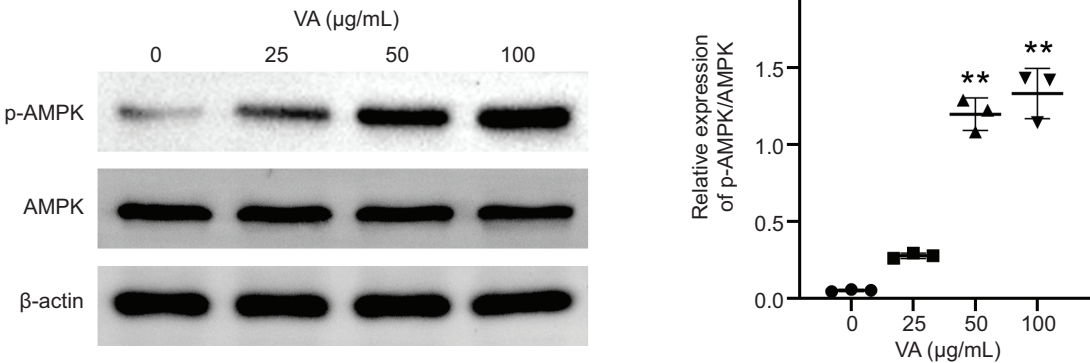


Figure 5. VA promotes the AMPK pathway activation. The levels of phosphorylated and non-phosphorylated AMPK were assessed using western blotting, with β-actin as the reference protein. Semi-quantitative analysis of phosphorylated and non-phosphorylated AMPK was conducted using ImageJ software. ***p* < 0.01 vs. 0 µg/mL VA group.

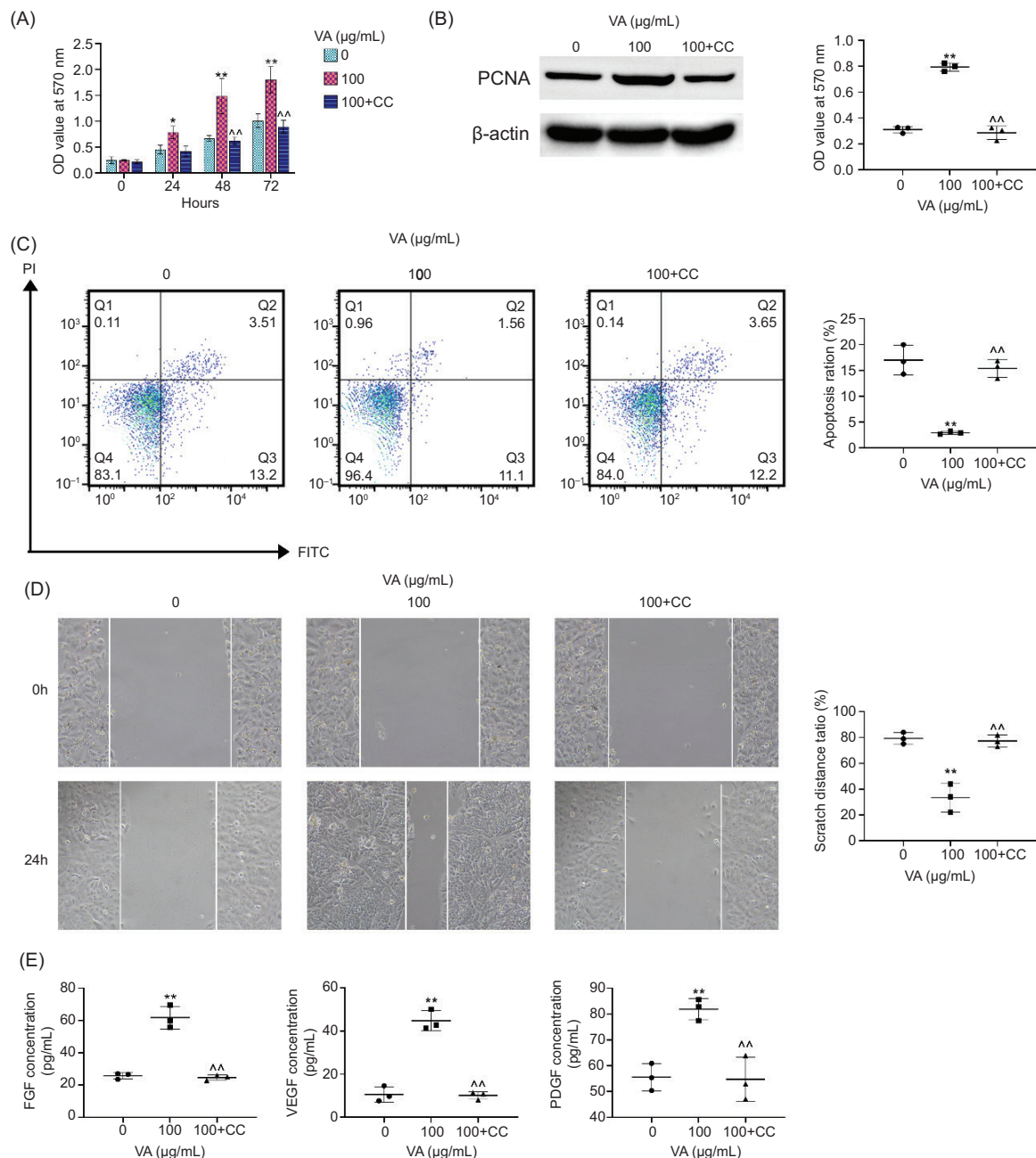


Figure 6. Inhibition of the AMPK pathway reverses the effects of VA on keratinocytes. (A) HaCaT cell proliferation was assessed using the MTT assay. Optical density (OD₅₇₀) values were measured at 0, 24, 48, and 72 h. (B) PCNA expression was determined by western blotting at 24 h. (C) Flow cytometry analysis of HaCaT cell apoptosis performed using Annexin V-FITC/PI staining at 24 h. (D) HaCaT cell migration was evaluated using an in vitro scratch assay, and width measurements were performed using ImageJ. (E) Secretion levels of FGF, PDGF, and VEGF were assessed using ELISA kits. ***p* < 0.01 vs. 0 µg/mL VA group. ^^vs. 100 µg/mL VA group.

with tissue remodeling and are critical for the migration of keratinocytes during wound healing (Hingorani *et al.*, 2018). As observed in this study, VA treatment induced the expression of MMP-2 and MMP-9, promoting the migration of keratinocytes and contributing to wound re-epithelialization. Moreover, VA enhanced the secretion

of key factors in angiogenesis, including FGF, VEGF, and PDGF, particularly in the early stages of wound healing.

Based on the findings presented above, VA was found to exhibit multifunctional properties in the processes of wound re-epithelialization and angiogenesis. However,

the precise mechanisms through which VA regulates these physiological processes remain unknown. Previous studies have established that the AMPK pathway can modulate the expression of apoptosis-related proteins such as Bax and Bcl-2, as well as the expression of MMP-2 and MMP-9 (Li *et al.*, 2017; Vilchinskaya *et al.*, 2023). VA treatment was shown to increase the protein levels of phosphorylated AMPK, indicating AMPK pathway activation by VA. This was further confirmed by the use of the AMPK inhibitor, CC, which reversed the effects of VA on cell proliferation, apoptosis, and migration. Taken together, the proposed mechanism of VA in wound healing may be as follows: VA activates the AMPK pathway, leading to the expression of a series of genes involved in cell proliferation, apoptosis, migration, and angiogenesis. Consequently, AMPK activation inhibits keratinocyte apoptosis while promoting their proliferation and migration. Furthermore, VA induces the secretion of FGF, VEGF and PDGF, thereby facilitating the angiogenesis process.

It is important to note that the HaCaT in vitro model may not fully replicate the complexity of in vivo conditions, which include intricate immune responses, hemostasis, and interactions with the ECM. Further in vivo studies are necessary to validate the efficacy of VA in wound healing. Additionally, given the observed effects of VA at relatively high concentrations in vitro, comprehensive safety assessments are required to evaluate potential side effects associated with high dosages.

In conclusion, the findings from this study indicate that VA may enhance wound healing by promoting keratinocyte proliferation, migration, and angiogenesis.

Availability of Data and Materials

All data generated or analyzed during this study are included in this published article.

The datasets used and/or analyzed during the present study are available from the corresponding author on reasonable request.

Conflict of Interest

The authors declare no conflict of interest.

Author Contributions

All authors contributed to the study's conception and design. Material preparation and experiments were performed by X.Z. Data collection and analysis were

performed by J.M. The first draft of the manuscript was written by J.H., with all authors providing feedback on previous versions. All authors read and approved the final manuscript.

References

- Bai, F., Fang, L., Hu, H., Yang, Y., Feng, X., & Sun, D. (2019). Vanillic acid mitigates the ovalbumin (OVA)-induced asthma in rat model through prevention of airway inflammation. *Biosci Biotechnol Biochem*, 83(3), 531–537. <https://doi.org/10.1080/09168451.2018.1543015>
- Cabral-Pacheco, G.A., Garza-Veloz, I., Castruita-De la Rosa, C., Ramirez-Acuña, J.M., Perez-Romero, B.A., Guerrero-Rodriguez, J.F., Martinez-Avila, N., & Martinez-Fierro, M.L. (2020). The Roles of Matrix Metalloproteinases and Their Inhibitors in Human Diseases. *International Journal of Molecular Sciences*, 21(24), 9739. <https://www.mdpi.com/1422-0067/21/24/9739>
- Dekoninck, S., & Blanpain, C. (2019). Stem cell dynamics, migration and plasticity during wound healing. *Nature Cell Biology*, 21(1), 18–24. <https://doi.org/10.1038/s41556-018-0237-6>
- Fang, W.-C., & Lan, C.-C. E. (2023). The Epidermal Keratinocyte as a Therapeutic Target for Management of Diabetic Wounds. *International Journal of Molecular Sciences*, 24(5), 4290. <https://www.mdpi.com/1422-0067/24/5/4290>
- Gong, J., Zhou, S., & Yang, S. (2019). Vanillic Acid Suppresses HIF-1 α expression via Inhibition of mTOR/p70S6K/4E-BP1 and Raf/MEK/ERK pathways in human colon cancer HCT116 cells. *International Journal of Molecular Sciences*, 20(3). <https://doi.org/10.3390/ijms20030465>
- Gonzalez, A.C., Costa, T.F., Andrade, Z.A., & Medrado, A.R. (2016). Wound healing - a literature review. *Anais Brasileiros de Dermatologia*, 91(5), 614–620. <https://doi.org/10.1590/abd1806-4841.20164741>
- Hegde, A., Ananthan, A.S.H.P., Kashyap, C., & Ghosh, S. (2021). Wound healing by keratinocytes: a cytoskeletal perspective. *Journal of the Indian Institute of Science*, 101(1), 73–80. <https://doi.org/10.1007/s41745-020-00219-9>
- Hingorani, D.V., Lippert, C.N., Crisp, J.L., Savariar, E.N., Hasselmann, J.P.C., Kuo, C., Nguyen, Q.T., Tsien, R.Y., Whitney, M.A., & Ellies, L.G. (2018). Impact of MMP-2 and MMP-9 enzyme activity on wound healing, tumor growth and RACPP cleavage. *PLoS One*, 13(9), e0198464. <https://doi.org/10.1371/journal.pone.0198464>
- Jeong, H.J., Nam, S.Y., Kim, H.Y., Jin, M.H., Kim, M.H., Roh, S.S., & Kim, H.M. (2018, Dec). Anti-allergic inflammatory effect of vanillic acid through regulating thymic stromal lymphopoietin secretion from activated mast cells. *Natural Product Research*, 32(24), 2945–2949. <https://doi.org/10.1080/14786419.2017.1389938>
- Kaur, J., Gulati, M., Singh, S.K., Kuppusamy, G., Kapoor, B., Mishra, V., Gupta, S., Arshad, M.F., et al. (2022). Discovering multifaceted role of vanillic acid beyond flavours: nutraceutical and therapeutic potential. *Trends in Food Science & Technology*, 122, 187–200. <https://doi.org/https://doi.org/10.1016/j.tifs.2022.02.023>

- Li, W.-D., Li, N.-P., Song, D.-D., Rong, J.-J., Qian, A.-M., & Li, X.-Q. (2017). Metformin inhibits endothelial progenitor cell migration by decreasing matrix metalloproteinases, MMP-2 and MMP-9, via the AMPK/mTOR/autophagy pathway. *International Journal of Molecular Medicine*, 39(5), 1262–1268. <https://doi.org/10.3892/ijmm.2017.2929>
- Ma, Z., Huang, Z., Zhang, L., Li, X., Xu, B., Xiao, Y., Shi, X., Zhang, H., et al. (2020). Vanillic acid reduces pain-related behavior in knee osteoarthritis rats through the inhibition of NLRP3 inflammasome-related synovitis. *Frontiers in Pharmacology*, 11, 599022. <https://doi.org/10.3389/fphar.2020.599022>
- Natewong, S., Niwaspragrit, C., Ratanachamnong, P., Samatiwat, P., Namchaiw, P., & Jaisin, Y. (2022). Photo-protective and anti-inflammatory effects of antidesma thwaitesianum müll. arg. fruit extract against UVB-Induced Keratinocyte Cell Damage. *Molecules*, 27(15). <https://doi.org/10.3390/molecules27155034>
- Oluwole, D.O., Coleman, L., Buchanan, W., Chen, T., La Ragione, R.M., & Liu, L.X. (2022). Antibiotics-free compounds for chronic wound healing. *Pharmaceutics*, 14(5). <https://doi.org/10.3390/pharmaceutics14051021>
- Pastar, I., Stojadinovic, O., Yin, N.C., Ramirez, H., Nusbaum, A.G., Sawaya, A., Patel, S.B., et al. (2014). Epithelialization in wound healing: a comprehensive review. *Advances in Wound Care* 3(7), 445–464. <https://doi.org/10.1089/wound.2013.0473>
- Qian, W., Yang, M., Wang, T., Sun, Z., Liu, M., Zhang, J., Zeng, Q., Cai, C., & Li, Y. (2020). Antibacterial mechanism of vanillic acid on physiological, morphological, and biofilm properties of carbapenem-resistant enterobacter hormaechei. *Journal of Food Protection*, 83(4), 576–583. <https://doi.org/https://doi.org/10.4315/JFP-19-469>
- Rakita, A., Nikolić, N., Mildner, M., Matiassek, J., & Elbe-Bürger, A. (2020). Re-epithelialization and immune cell behaviour in an ex vivo human skin model. *Scientific Reports*, 10(1), 1. <https://doi.org/10.1038/s41598-019-56847-4>
- Rousselle, P., Braye, F., & Dayan, G. (2019). Re-epithelialization of adult skin wounds: cellular mechanisms and therapeutic strategies. *Advanced Drug Delivery Reviews*, 146, 344–365. <https://doi.org/https://doi.org/10.1016/j.addr.2018.06.019>
- Salau, V.F., Erukainure, O.L., Ibeji, C.U., Olasehinde, T.A., Koorbanally, N.A., & Islam, M.S. (2020). Vanillin and vanillic acid modulate antioxidant defense system via amelioration of metabolic complications linked to Fe(2+)-induced brain tissues damage. *Metabolic Brain Disease*, 35(5), 727–738. <https://doi.org/10.1007/s11011-020-00545-y>
- Ullah, R., Ikram, M., Park, T.J., Ahmad, R., Saeed, K., Alam, S.I., Rehman, I.U., Khan, A., Khan, I., Jo, M.G., & Kim, M.O. (2020). Vanillic acid, a bioactive phenolic compound, counteracts lps-induced neurotoxicity by regulating c-Jun N-terminal kinase in mouse brain. *International Journal of Molecular Sciences*, 22(1). <https://doi.org/10.3390/ijms22010361>
- Vilchinskaya, N.A., Rozhkov, S.V., Turtikova, O.V., Mirzoev, T.M., & Shenkman, B.S. (2023). AMPK phosphorylation impacts apoptosis in differentiating myoblasts isolated from atrophied rat soleus muscle. *Cells*, 12(6), 920. <https://www.mdpi.com/2073-4409/12/6/920>
- Yao, X., Jiao, S., Qin, M., Hu, W., Yi, B., & Liu, D. (2020). Vanillic acid alleviates acute myocardial hypoxia/reoxygenation injury by inhibiting oxidative stress. *Oxidative Medicine and Cellular Longevity*, 2020, 8348035. <https://doi.org/10.1155/2020/8348035>